

## Charge-sharing dynamics of dissociating highly charged ions

J. Matsumoto ,\* Y. Iwasaki, and H. Shiromaru

*Department of Chemistry, Tokyo Metropolitan University, Hachioji, Tokyo 192-0397, Japan*

G. Veshapidze 

*Faculty of Business, Technology and Education, Ilia State University, Tbilisi 0162, Georgia*



(Received 29 March 2020; accepted 4 August 2020; published 31 August 2020)

Low-energy collision experiments of  $\text{Ar}^{8+}$  with acetylene ( $\text{C}_2\text{H}_2$ ) molecules were conducted, and four-body dissociation of highly ionized acetylene was studied focusing on charge-sharing dynamics in two dissociating carbon (C) ions. When the C ions shared three positive charges, the kinetic energy distributions of the two terminal protons, one from the near-site carbon detected as  $\text{C}^{2+}$  and the other from the other site, were quite similar, indicating equal sharing of the charges by the two C atoms until the C-C bond was elongated to at least about 200 pm. When the carbons had four positive charges to be shared after dissociation by a  $\text{C}^{3+}$  and a  $\text{C}^+$  pair, the kinetic energy of the  $\text{H}^+$  ion from the 3+ site was higher than its counterpart, while the difference was much smaller than the pure Coulombic value for  $\text{C}^{3+}$  and  $\text{C}^+$  sharing from the beginning of dissociation.

DOI: [10.1103/PhysRevA.102.022819](https://doi.org/10.1103/PhysRevA.102.022819)

### I. INTRODUCTION

When a multiply ionized molecule dissociates into fragment ions, for example by ionization and Coulomb explosion processes as represented by the reaction  $\text{AB} \rightarrow \text{AB}^{(m+n)+} + (m+n)e^- \rightarrow \text{A}^{m+} + \text{B}^{n+} + (m+n)e^-$ , the transient positive charges on the dissociating A and B atoms may be different from those after dissociation. Theoretically, the time evolution of the effective charge of the dissociating fragment, namely the charge-sharing dynamics, may be obtained from the variation of the wave functions with internuclear distance. Experimentally, for example in collision experiments, multiple ionization usually yields molecular ions in various electronic states, which dissociate according to their own potential curves with different charge-sharing schemes [1]. To understand the dissociation process while avoiding complexity, a semiclassical Coulomb explosion model has been adopted, in which the processes that depend on various electronic states are coarse grained.

Although the pure Coulomb explosion model places point charges on the atoms and hence involves oversimplification, it has been successfully applied to determine molecular structures [2] and orientations [3]. It is not suitable for highly accurate determination, but it can be a powerful tool for finding the correct option among a limited variety of structures, such as for enantiomers [4,5]. Elucidation of the charge-sharing dynamics will enable understanding of a more detailed picture of dissociation within the framework of the pure Coulomb explosion model.

If the internuclear distance is fairly large, charge sharing is nearly fixed from the beginning when ionization occurs. For example, when  $\text{Ar}_2$  is fourfold ionized by low-energy

collision with a highly charged ion, 3 + 1 sharing events of 4+ charge ( $\text{Ar}_2^{4+} \rightarrow \text{Ar}^{3+} + \text{Ar}^+$ ) are more abundant than 2 + 2 sharing events [6], in which a higher-charged fragment is preferentially formed at the near site of the projectile [7]. This is a typical outcome of the large internuclear distance of  $\text{Ar}_2$  (380 pm), i.e., the absence, or inefficiency, of charge redistribution processes. This is not the case for molecules with covalent bonds, where electrons are initially shared by two atoms and charge redistribution may occur during dissociation [8]. Then simple questions arise: When is the final charge sharing fixed on average, and what is the critical internuclear distance for this?

In the pure Coulomb explosion model, the linear momenta of the fragment ions are given by the time integral of the Coulomb repulsion force. Consequently, the kinetic energies of the fragment ions may reflect the charge sharing history. For example, the Coulomb repulsion in triply ionized diatomic molecules is larger for the equal-sharing case ( $1.5 \times 1.5 > 2 \times 1$ ) and consequently the kinetic energies of the fragments will also be higher compared to the unequal-charge-sharing case. However, it is difficult to judge the charge-sharing pattern based solely on kinetic energy measurements, because the repulsive potential curves are different among the various electronic states produced in the ionization event. That is, a kinetic energy higher than the Coulombic value does not provide sufficient evidence that the molecule started to dissociate with equal charge sharing.

Dissociation of highly ionized acetylene ( $\text{C}_2\text{H}_2^{n+}$ ,  $n \geq 5$ ) offers an opportunity to determine this critical distance using quickly dissociating  $\text{H}^+$  ions as a probe. In dissociation yielding four atomic ions, the two  $\text{H}^+$  ions are pushed by the Coulomb force from inner C ions, and the charge-sharing history of the inner C ions affects the final kinetic energies of the  $\text{H}^+$  ions. The kinetic energy difference between the two  $\text{H}^+$  ions depends on when the C ions become charge

\*Corresponding author: [junmatsu@tmu.ac.jp](mailto:junmatsu@tmu.ac.jp)

asymmetric. The advantage of this approach lies in observing the symmetry of the energies of the two  $H^+$  ions, instead of the absolute values of the kinetic energies, to sensitively detect the charge asymmetry in the C ions.

Multiple ionization followed by ionic dissociation of acetylene has been intensively studied using various ionization methods, for example, through ion impact [9–12], x-ray irradiation [13], and intense laser [14–18] and free-electron laser [19,20] ionization. The motivation for studying this molecule lies mainly in its linear molecular structure and the fact that it is the smallest hydrocarbon molecule, which are advantageous characteristics for observing charge-sharing dynamics.

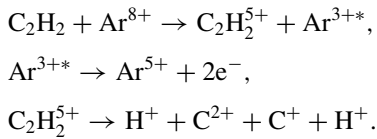
In the present study, acetylene was highly ionized by low-energy (3 keV/u) collision of  $Ar^{8+}$ , in which the main ionization mechanism is multiple electron capture. For the specific dissociation channels, the velocity vectors of the four fragment ions were analyzed. A critical internuclear distance, until which the charge sharing can be regarded as symmetric, or less asymmetric than the final sharing, is obtained from the kinetic energies of the  $H^+$  ions with the aid of numerical simulations based on the pure Coulomb explosion model.

## II. EXPERIMENT

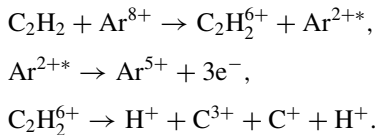
We used apparatus previously employed for  $Ar^{8+}$ -ethylene low-energy collision experiments [21]. A 120 keV  $Ar^{8+}$  beam extracted from an electron cyclotron resonance ion source [22] was injected into the collision chamber, where the target  $C_2H_2$  gas was introduced from a beam-source chamber and trimmed with a skimmer. In the collision chamber, the target beam crossed the  $Ar^{8+}$  beam and eventually made contact with the surface of a liquid-nitrogen-cooled trap. A typical operational pressure of  $2 \times 10^{-5}$  Pa was used on the collision chamber.

Position sensitive time-of-flight (PSTOF) measurements were conducted for the recoil ions, with detection of scattered  $Ar^{5+}$  acting as the start trigger. The following reactions were analyzed in detail:

(1) Five-electron capture: The projectile emits two Auger electrons after collision, and the recoil ion dissociates into four atomic ions, hereafter referred to as the (1,2,1,1) channel:



(2) Six-electron capture: The projectile emits three Auger electrons, and dissociation via the (1,3,1,1) channel:



In this paper, the H site near the carbon to be detected as  $C^{2+}$  (or  $C^{3+}$ ) will be referred to as the “2+ (or 3+) site,” and the counterpart will be referred to as the “1+ site.” The fourfold coincidence events for  $C_2H_2^{n+}$  ( $n \geq 7$ ) were not sufficiently obtained in the present setup.

In the analyses, events in which two ions were detected within 30 ns from each other were excluded. Thus, the

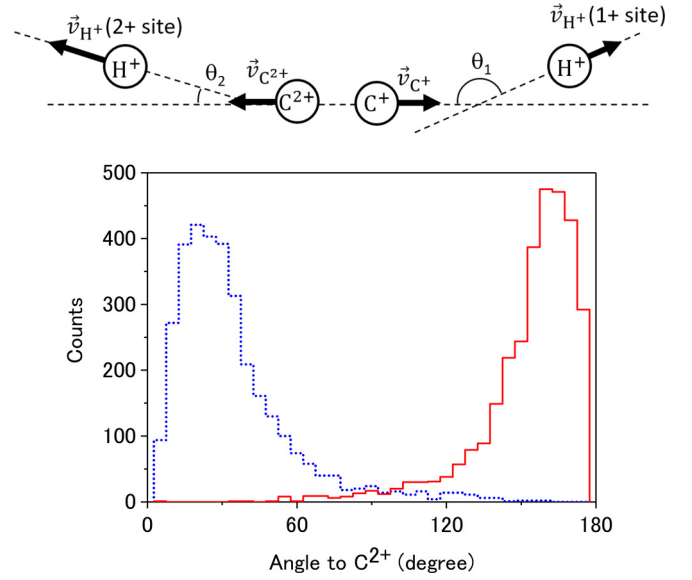


FIG. 1. Distribution of the angles between the  $C^{2+}$  and  $H^+$  velocity vectors. The top of the figure is a schematic of the vector correlation among the fragments. For two  $H^+$ s detected in coincidence, the ion with the smaller  $\theta$  is shown in blue dotted line and the other in solid red line. The minor events for the angles between  $60^\circ$  and  $120^\circ$  are excluded from further analysis.  $H^+$  ions in the small angle area are allocated to the 2+ site and those in large angle area are allocated to the 1+ site.

collision events in which the target molecules were oriented in the plane perpendicular to the TOF axis were excluded. The three-dimensional momentum-conservation restriction was imposed on the fragments for each event, whereas momentum transferred by the projectile was neglected.

## III. SIMULATION OF THE KINETIC ENERGIES OF THE FRAGMENTS

To analyze the charge-sharing dynamics, ion kinetic energies were simulated using a code based on the Coulomb explosion model. The code solves coupled second-order ordinary differential equations of motion for four point charges in three dimensions, interacting with each other by Coulomb forces:

$$\frac{d^2 \vec{r}_i}{dt^2} = \kappa \frac{q_i}{m_i} \sum_{\substack{k=1 \\ k \neq i}}^4 \frac{q_k}{|\vec{r}_i - \vec{r}_k|^3} (\vec{r}_i - \vec{r}_k),$$

where  $\vec{r}_i$ ,  $m_i$ , and  $q_i$  are the position, mass, and charge of the  $i$ th fragment, respectively, and  $\kappa$  is the Coulomb constant. This set of equations was numerically solved using the Runge-Kutta Prince-Dormand method, implemented in the GNU Scientific Library (GSL) [23]. The simulation started with a given initial charge sharing, and at a specific C-C distance (critical distance) the sharing was finalized. Although such a sudden change is not possible in reality, this approximation reflects the typical behavior of the dissociating ion pair. In other words, the simulation does not aim to reproduce event-by-event asymmetry.

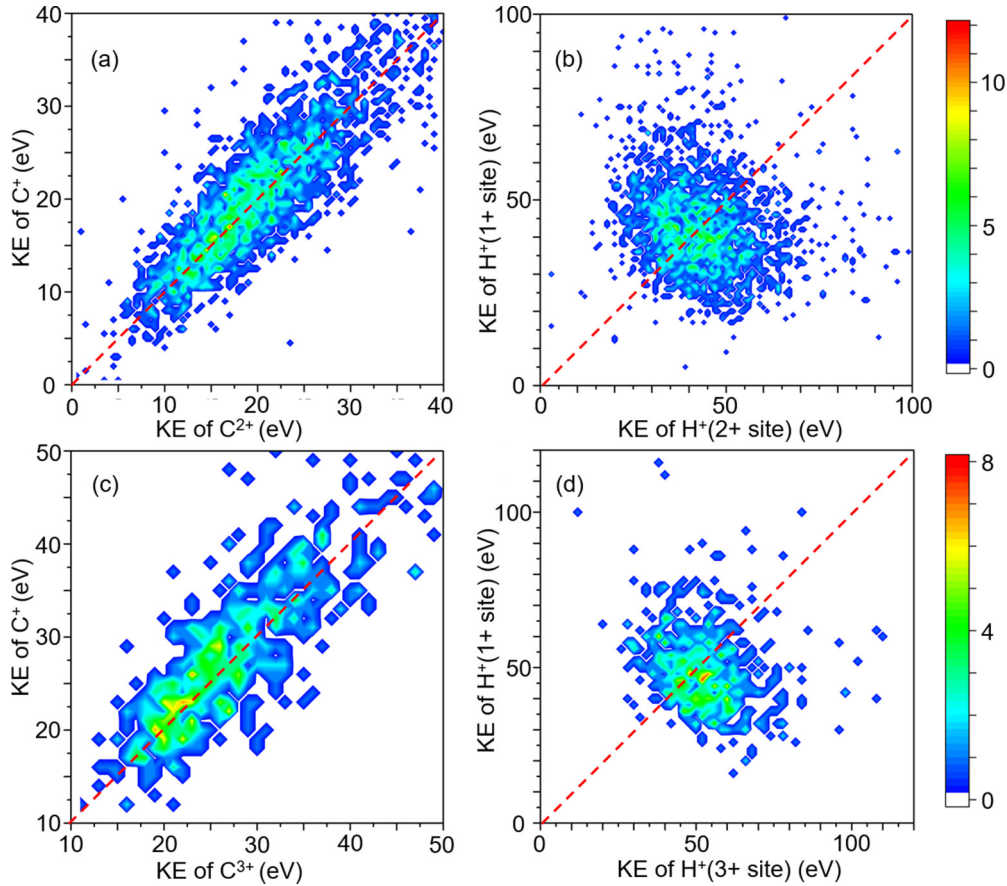


FIG. 2. Correlations of the kinetic energies for the (1,2,1,1) channel: (a)  $C^{2+}/C^+$  pair and (b)  $H^+(2+ \text{ site})/H^+(1+ \text{ site})$  pair. Those for the (1,3,1,1) channel are also shown: (c)  $C^{3+}/C^+$  pair and (d)  $H^+(3+ \text{ site})/H^+(1+ \text{ site})$  pair. Dashed lines indicate the case of equal kinetic energies. Units of the color scales are (a) counts/ $(0.5 \text{ eV})^2$ , (b) counts/ $(1 \text{ eV})^2$ , (c) counts/ $(1 \text{ eV})^2$ , (d) counts/ $(2 \text{ eV})^2$ .

The time step was not greater than 0.1 fs, and if an iteration of the differential equations required a smaller time step, the algorithm would automatically use a smaller value to achieve the required convergence level. The kinetic energies at the end of the simulation (at  $t = 500$  fs), when the fractional change in relative velocity between C ions was less than  $4 \times 10^{-6}/\text{fs}$ , were regarded as the final kinetic energies. The validity of this procedure was confirmed by calculating the dissociation of  $H_2^{2+}$ . Final kinetic energies were calculated for varying critical distance.

## IV. RESULTS AND DISCUSSION

### A. Experimental results

The TOF spectra and multihit coincidence maps obtained in the present study are consistent with those reported previously [10]. The (1,2,1,1) and (1,3,1,1) channels were extracted from the four-hit events. In the fourfold coincidence analysis, the background signals (false coincidence events) were removed, and the relevant channels were well separated from the others.

The initial  $H^+$  sites were allocated by analyzing the vector correlations of dissociating fragments. Figure 1 presents a histogram of the angles between the  $H^+$  and  $C^{2+}$  velocity vectors for the (1,2,1,1) channel, together with a schematic of the vector correlation among the fragments. As expected from

the linear structure of acetylene at equilibrium, the distribution shows peaks around  $0^\circ$  and  $180^\circ$ . Considering that the volume element of the angle is small in this area, the preference is fairly strong, indicating that the Coulomb explosion model is valid. By excluding minor events for the angles between  $60^\circ$  and  $120^\circ$ , we can safely allocate  $H^+$  ions with an angle close to  $0^\circ$  as 2+ sites and those near  $180^\circ$  as 1+ sites. This procedure was also successfully applied to the (1,3,1,1) channel.

A strong correlation between kinetic energies of  $C^{2+}-C^+$  pairs is observed, as shown in Fig. 2(a), reflecting near two-body dissociation. In the classical picture, if a carbon ion pair has a large energy, the two  $H^+$  ions are kicked further resulting in a correlated increase in the kinetic energies of the  $H^+$ 's. However, no correlation is seen for the  $H^+-H^+$  pairs, as shown in Fig. 2(b), probably due to fast escape from the repulsive field. The symmetric shape of the island with respect to the dashed line indicates that the energy distributions of the two  $H^+$  ions are similar to each other.

The correlations of the kinetic energies of the  $C^{3+}-C^+$  pair and the  $H^+-H^+$  pair for the (1,3,1,1) channel are shown in Figs. 2(c) and 2(d), respectively. As in the case of the (1,2,1,1) channel, the correlation is strong for the  $C^{3+}-C^+$  pair and absent for the  $H^+-H^+$  pair. In Fig. 2(d), the center of the island deviates from the dashed line, indicating that the average

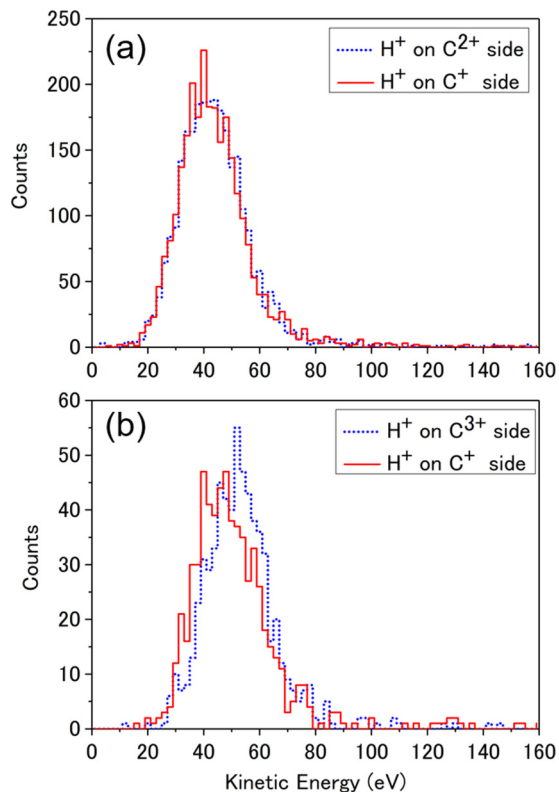


FIG. 3. (a) Kinetic energy distribution of  $H^+$  for the (1,2,1,1) channel. Those from near the  $C^{2+}$  site are shown by a blue dotted line, and those from near the  $C^+$  site are shown by a red solid line. (b) Those for the (1,3,1,1) channel.

kinetic energy of the  $H^+(3+ \text{ site})$  is slightly larger than that of the  $H^+(1+ \text{ site})$ .

The kinetic energy distributions obtained in the present study for the (1,2,1,1) and (1,3,1,1) channels are shown in Figs. 3(a) and 3(b), respectively. The two plots for the (1,2,1,1) channel are very similar to each other and both exhibit a maximum at around 40 eV. For the (1,3,1,1) channel, the kinetic energy distributions of the  $H^+(1+ \text{ site})$  and  $H^+(3+ \text{ site})$  show maxima at around 45 eV and around 50 eV, respectively. The kinetic energy distributions of  $H^+$  were reported previously for detected  $H^+ + H^+$  and  $H^+ + C^{n+}$  ( $n = 1-3$ ) ion pairs, and the most probable values of the energies were 18 eV ( $H^+ + C^+$ ), 40 eV ( $H^+ + C^{2+}$ ), and 54 eV ( $H^+ + C^{3+}$ ) [10]. The results shown in Figs. 3(a) and 3(b) agree well with those reported previously for the latter two channels, implying that the undetected species in the double-hit studies were ionic fragments. In contrast, the kinetic energies reported in Ref. [10] for the ( $H^+ + C^+$ ) channel were distributed in a much lower energy region than those in the present study, implying that the undetected species were mostly neutral.

In the pure Coulomb explosion model, the kinetic energy distribution is determined from the initial distribution of the internuclear distances of the molecule before ionization, undergoing zero-point vibrations. Briefly, it determines the widths of the distribution, whereas the charge asymmetry causes a difference in the average values. If the charge sharing is  $2 + 1$  from the beginning, the kinetic energy of the  $H^+(2+ \text{ site})$  would be about 8 eV higher than that of

the  $H^+(1+ \text{ site})$ , according to the pure Coulomb explosion model.

The near equality in the kinetic energy distribution indicates symmetric charge sharing of inner carbons, around  $1.5 + 1.5$ , until the two  $H^+$  ions have been sufficiently separated from  $C^{2+}$  and  $C^+$ . Taking statistical uncertainty into account, the difference between their peak positions is estimated to be  $0.77 \pm 0.57$  eV, namely 1.34 eV at the maximum, within a 90% confidence interval. It should be noted that the kinetic energy difference for the two  $H^+$  ions in each event has a wide variation. As shown in Fig. 2(b), in some events the kinetic energies of the  $H^+(2+ \text{ site})$  are about 40 eV higher than the other, and in some events they are about 40 eV lower; on average they are nearly the same.

A difference of about 17 eV should be observed between the kinetic energy distributions of the  $H^+$  ions in the (1,3,1,1) channel, if the sharing is  $3 + 1$  from the beginning, according to the pure Coulomb explosion model. The experimental value is much smaller:  $4.24 \pm 0.88$  eV within a 90% confidence interval. However, the difference is clearly visible, in contrast to the case of the (1,2,1,1) channel. The charge-sharing dynamics of  $(C_2)^{4+}$  are different from those of  $(C_2)^{3+}$  because two possible final sharing configurations,  $3 + 1$  and  $2 + 2$ , can be realized for the former. Because energetically unfavorable charge redistribution is suppressed, if the charge sharing was  $2 + 2$  at the beginning, the final products will likely be two  $C^{2+}$  ions. Thus, the initial charge sharing can be  $3 - \delta$  and  $1 + \delta$ , where  $\delta$  is a ‘‘charge equalizing factor’’ less than 1, corresponding to the nominal number of electrons transferred between two carbons during dissociation.

## B. Simulation of charge sharing

The simulated kinetic energies of the fragment ions for the (1,2,1,1) channel are shown in Fig. 4(a). The abscissa shows the C-C distance (critical distance) where the charge sharing changes from  $1.5 + 1.5$  to  $2 + 1$ . The values at the equilibrium geometry were adopted for the initial C-C and C-H distances: 120.3 and 106.0 pm, respectively. The simulated energies are slightly lower than the peak values of the experimental energy distributions.

Although the equilibrium geometry of  $C_2H_2$  is linear, the most probable bond angles deviate slightly due to zero-point vibration in the degenerate bending modes [24]. The curves obtained for several initial geometries including linear conformation and a  $20^\circ$  bend form with cis, trans, and  $90^\circ$  twisted conformations are shown in Fig. 4(b), where the vertical scale is magnified to show the difference. The initial geometry dependence is very small, with a difference of about 0.1 eV between the values for the linear geometry (upper curve) and those for the other three geometries, which cannot be resolved in Fig. 4(a).

The simulated kinetic energies of the fragment ions for the (1,3,1,1) channel are shown in Fig. 4(c). The initial charge sharing is tentatively set to be  $2.1 + 1.9$  ( $\delta = 0.9$ ). The validity of this  $\delta$  value is discussed later. As in the case of the (1,2,1,1) channel, the simulated energies are slightly lower than the peak values of the experimental energy distributions, and the initial geometry dependence is not resolved in this vertical scale.

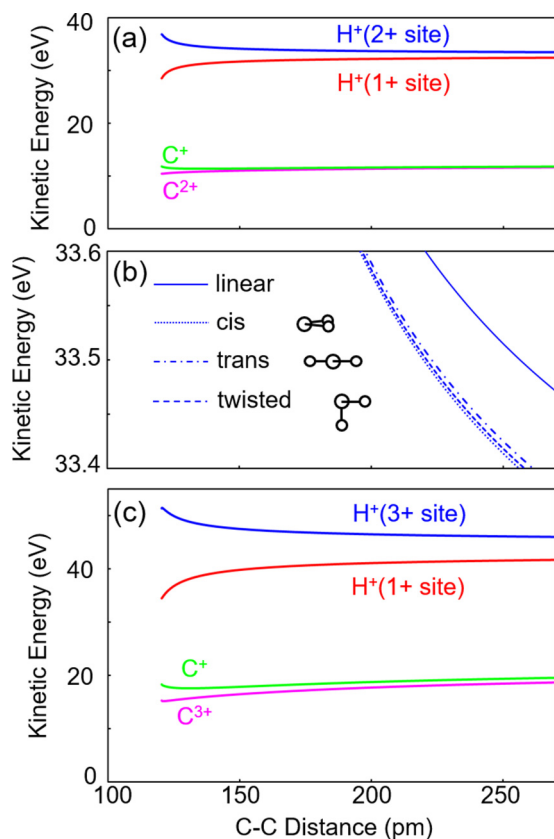


FIG. 4. Simulated kinetic energies of the fragment ions as a function of C-C distance where the charge sharing is finalized. (a) Those for the (1,2,1,1) channel with initial charge sharing of  $C^{1.5+}-C^{1.5+}$ . (b) Those for the (1,2,1,1) channel calculated with different initial geometries. Those starting from a linear conformation are shown by the solid curve, and those starting from  $20^\circ$ -bent C-C-H angles with dihedral angles of  $0^\circ$  (cis),  $90^\circ$  (twisted), and  $180^\circ$  (trans) are shown by dotted, dashed, and dot-dashed curves, respectively. The molecular structures of the latter three are shown schematically. The vertical scale is magnified ( $\times 200$ ). (c) Those for the (1,3,1,1) channel with initial charge sharing of  $C^{2.1+}-C^{1.9+}$ .

To visualize the asymmetry in the kinetic energies of  $H^+$  ions, the simulated kinetic energy differences ( $\Delta KE$ ) in the (1,2,1,1) and (1,3,1,1) channels are shown in Figs. 5(a) and 5(b), respectively. The curves for several initial geometries seem almost the same on these vertical scales. For the (1,2,1,1) channel, the value of  $\Delta KE$  rapidly decreases in the first 10 pm elongation of the C-C distance with equal sharing. If the charge sharing is finalized at 3 fs after the ionization (at about 128 pm of the C-C distance), the value of  $\Delta KE$  drops to 50% of the value for the 2 + 1 sharing from the beginning. The experimentally obtained maximum  $\Delta KE$  is 1.34 eV. Thus, the charge sharing is finalized at a C-C distance longer than about 200 pm, at least 9–10 fs after ionization.

For the (1,3,1,1) channel, setting  $\delta = 0.9$  in the simulation leads to a similar critical distance to reproduce the experimental  $\Delta KE$ . In contrast, for  $\delta = 0.75$ , the simulated value of  $\Delta KE$  is always larger than the experimental values. Because a smaller value of  $\delta$ , namely a more asymmetric start, will be

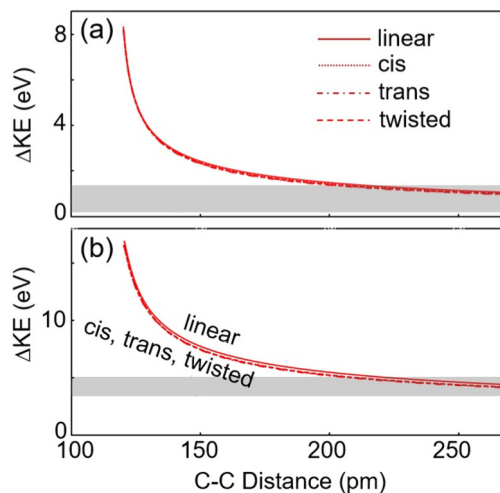


FIG. 5. (a) Plot of the simulated kinetic energy differences between  $C^+$  site  $H^+$  and  $C^{2+}$  site  $H^+$  ( $\Delta KE$ ), and (b) that for  $C^+$  site  $H^+$  and  $C^{3+}$  site  $H^+$ , as a function of the C-C distance where the charge sharing is finalized. The shaded areas represent the experimental values within a 90% confidence interval.

incorporated into longer critical distances, these values cannot be fixed solely from the energy difference. However, we can safely conclude that the charge sharing at the beginning of dissociation is nearly symmetric.

## V. CONCLUSION

Here, we demonstrate the asymmetry in the kinetic energies of  $H^+$  ions reflects the charge-sharing dynamics of C ions. For the (1,2,1,1) channel, charge sharing is not fixed until the C-C distance is approximately doubled. For the (1,3,1,1) channel, charge sharing is nearly symmetric and not fixed until C-C distance becomes considerably longer. This Coulomb explosion model should be investigated for other molecules using the kinetic energy difference among the peripheral hydrogen atoms as a probe. The charge-sharing dynamics for dissociation channels involving higher-charged fragment ions remain for further study.

Finally, it should be noted that the bird's-eye view obtained in the present study is complementary to the state-selective approach. The charge-sharing scheme explored here can be made more realistic by adopting time-dependent screening of the nuclear charges of the dissociating ions. For the state-selective approach, the asymmetry in the kinetic energies should be reproduced by analyzing dissociative potential surfaces for the various electronic states of the transient highly ionized parent molecules, accurately in principle. That is, the observed asymmetry, or absence thereof, will provide a good benchmark for theoretical calculations of dissociating highly ionized molecules.

## ACKNOWLEDGMENTS

G. V. was supported by a followup program for overseas Ph.D. students of Tokyo Metropolitan University.

- [1] For example, M. Tarisien, L. Adoui, F. Frémont, D. Lelièvre, L. Guillaume, J.-Y. Chesnel, H. Zhang, A. Dubois, D. Mathur, S. Kumar, M. Krishnamurthy, and A. Cassimi, *J. Phys. B: At. Mol. Opt. Phys.* **33**, L11 (2000).
- [2] Z. Vager, R. Naaman, and E. P. Kanter, *Science* **244**, 426 (1989).
- [3] B. Siegmann, U. Werner, R. Mann, Z. Kaliman, N. M. Kabachnik, and H. O. Lutz, *Phys. Rev. A* **65**, 010704(R) (2001).
- [4] T. Kitamura, T. Nishide, H. Shiromaru, Y. Achiba, and N. Kobayashi, *J. Chem. Phys.* **115**, 5 (2001).
- [5] M. Pitzer, M. Kunitski, A. S. Johnson, T. Jahnke, H. Sann, F. Sturm, L. Ph. H. Schmidt, H. Schmidt-Böcking, R. Dörner, J. Stohner, J. Kiedrowski, M. Reggelin, S. Marquardt, A. Schießer, R. Berger, and M. S. Schöffler, *Science* **341**, 1096 (2013).
- [6] J. Matsumoto, A. Leredde, X. Flechard, K. Hayakawa, H. Shiromaru, J. Rangama, C. L. Zhou, S. Guillous, D. Hennecart, T. Muranaka, A. Mery, B. Gervais, and A. Cassimi, *Phys. Rev. Lett.* **105**, 263202 (2010).
- [7] W. Iskandar, J. Matsumoto, A. Leredde, X. Flechard, B. Gervais, S. Guillous, D. Hennecart, A. Mery, J. Rangama, C. L. Zhou, H. Shiromaru, and A. Cassimi, *Phys. Rev. Lett.* **113**, 143201 (2014).
- [8] M. Ehrich, U. Werner, H. O. Lutz, T. Kaneyasu, K. Ishii, K. Okuno, and U. Saalman, *Phys. Rev. A* **65**, 030702(R) (2002).
- [9] S. De, J. Rajput, A. Roy, P. N. Ghosh, and C. P. Safvan, *J. Chem. Phys.* **127**, 051101 (2007).
- [10] S. De, J. Rajput, A. Roy, P. N. Ghosh, and C. P. Safvan, *Phys. Rev. A* **77**, 022708 (2008).
- [11] T. Mizuno, T. Yamada, H. Tsuchida, Y. Nakai, and A. Itoh, *J. Phys.: Conf. Ser.* **163**, 012039 (2009).
- [12] J. Rajput, A. Agnihotri, A. Cassimi, X. Fléchar, S. Guillous, W. Iskandar, A. Méry, J. Rangama, and C. P. Safvan, *J. Phys.: Conf. Ser.* **875**, 102003 (2017).
- [13] T. Osipov, C. L. Cocke, M. H. Prior, A. Landers, Th. Weber, O. Jagutzki, L. Schmidt, H. Schmidt-Böcking, and R. Dörner, *Phys. Rev. Lett.* **90**, 233002 (2003).
- [14] A. Hishikawa, A. Matsuda, M. Fushitani, and E. J. Takahashi, *Phys. Rev. Lett.* **99**, 258302 (2007).
- [15] X. Gong, Q. Song, Q. Ji, H. Pan, J. Ding, J. Wu, and H. Zeng, *Phys. Rev. Lett.* **112**, 243001 (2014).
- [16] S. Roither, X. Xie, D. Kartashov, L. Zhang, M. Schöffler, H. Xu, A. Iwasaki, T. Okino, K. Yamanouchi, A. Baltuska, and M. Kitzler, *Phys. Rev. Lett.* **106**, 163001 (2011).
- [17] Q. Song, X. Gong, Q. Ji, K. Lin, H. Pan, J. Ding, H. Zeng, and J. Wu, *J. Phys. B: At. Mol. Opt. Phys.* **48**, 094007 (2015).
- [18] N. Mitsubayashi, T. Yatsushashi, H. Tanaka, S. Furukawa, M. Kozaki, K. Okada, and N. Nakashima, *Int. J. Mass Spectrom.* **403**, 43 (2016).
- [19] Y. H. Jiang, A. Senftleben, M. Kurka, A. Rudenko, L. Foucar, O. Herrwerth, M. F. Kling, M. Lezius, J. V. Tilborg, A. Belkacem, K. Ueda, D. Rolles, R. Treusch, Y. Z. Zhang, Y. F. Liu, C. D. Schröter, J. Ullrich, and R. Moshhammer, *J. Phys. B: At. Mol. Opt. Phys.* **46**, 164027 (2013).
- [20] H. Ibrahim, B. Wales, S. Beaulieu, B. E. Schmidt, N. Thiré, E. P. Fowe, É. Bisson, C. T. Hebeisen, V. Wanie, M. Giguère, J.-C. Kieffer, M. Spanner, A. D. Bandrauk, J. Sanderson, M. S. Schuurman, and F. Légaré, *Nat. Commun.* **5**, 4422 (2014).
- [21] K. Takahashi, K. Yokokawa, A. Mizumura, J. Matsumoto, H. Shiromaru, H. Kumar, P. Bhatt, and C. P. Safvan, *Phys. Rev. A* **98**, 062708 (2018).
- [22] H. Tanuma, J. Matsumoto, T. Nishide, H. Shiromaru, and N. Kobayashi, *J. Chin. Chem. Soc.* **48**, 389 (2001).
- [23] <http://www.gnu.org>.
- [24] S. Hsieh and J. H. D. Eland, *J. Phys. B: At. Mol. Opt. Phys.* **30**, 4515 (1997).